Profiles of photosynthetically active radiation, nitrogen and photosynthetic capacity in the boreal forest: Implications for scaling from leaf to canopy

Qing Lai Dang,[1,2,3] Hank A. Margolis,[1,2] Mikailou Sy,[1,4] Marie R. Coyea,[1] G. James Collatz,[2] and Charles L. Walthall[5]

Abstract. Profiles of photosynthetically active radiation (PAR), leaf nitrogen per unit leaf area (N_{area}), and photosynthetic capacity (A_{max}) were measured in an aspen, two jack pine, and two black spruce stands in the BOREAS northern study area. N_{area} decreased with decreasing %PAR in each stand, in all conifer stands combined ($r = 0.52$) and in all stands combined ($r = 0.46$). Understory alder had higher N_{area} for similar %PAR than did aspen early in the growing season. A_{max} decreased with decreasing N_{area}, except for the negative correlation between N_{area} and A_{max} during shoot flush for jack pine. For the middle and late growing season data, N_{area} and A_{max} had r values of 0.51 for all stands combined and 0.60 for all conifer stands combined. For similar N_{area} the aspen stand had higher A_{max} than did the conifer stands. Photosynthetic capacity expressed as a percentage of A_{max} at the top of the canopy ($\%A_{max0}$) decreased with %PAR similarly in all stands, but $\%A_{max0}$ decreased at a much slower rate than did %PAR. To demonstrate the implications of the vertical distribution of A_{max}, three different assumptions were used to scale leaf A_{max} to the canopy ($A_{can-max}$): (1) constant A_{max} with canopy depth, (2) A_{max} scaled proportionally to %PAR, and (3) a linear relationship between A_{max} and cumulative leaf area index derived from our data. The first and third methods resulted in similar $A_{can-max}$; the second was much lower. All methods resulted in linear correlations between normalized difference vegetation indices measured from a helicopter and $A_{can-max}$ ($r = 0.97, 0.93$, and 0.97, respectively), but the slope was strongly influenced by the scaling method.

Introduction

Most measurements and knowledge of photosynthesis for boreal forest trees are at the level of individual leaves or branches. For modeling the carbon balance of the boreal forest at landscape, regional, and continental scales, therefore, it is useful if easily measured leaf-level parameters can be integrated reliably, simply, and realistically both vertically through the canopy and horizontally across different components of the landscape. There have been a number of attempts in recent years to scale photosynthesis from leaf to canopy [*Hirose and Werger*, 1987a; *Charles-Edwards et al.*, 1987; *Wang and Jarvis*, 1991; *Evans and Farquhar*, 1991; *Sellers et al.*, 1992, 1996; *Norman*, 1993; *Luo et al.*, 1994; *Schulze et al.*, 1994; *Kull and Jarvis*, 1995]. For regional and global scale carbon-modeling applications, certain simplifying assumptions are made concerning the vertical distribution of photosynthetic capacity within plant canopies [e.g., *Sellers et al.*, 1992, 1996; *Kull and*

Jarvis, 1995]. Deviations of the assumed distribution from the actual distribution can potentially cause errors in the estimation of canopy photosynthesis and primary productivity.

A set of ecophysiological principles has been proposed that generalizes the relationship between the CO_2-fixing capacity of a canopy, the nitrogen concentration of foliage, the amount of photosynthetically active radiation (PAR) that the canopy absorbs, and the vertical distribution of photosynthetic capacity within plant canopies [*Field and Mooney*, 1986, 1991; *Farquhar*, 1989]. These principles are based on the idea that natural selection has acted on plant communities in such a way that the investment of resources in CO_2 fixation capacity is optimized for a given level of resource availability. Consequently, it follows that there should be a relationship between light availability and CO_2 fixation capacity that is relatively consistent across a range of species [*Mooney and Gulmon*, 1979, 1982; *Bloom et al.*, 1985]. *Field* [1991] refers to this phenomenon as functional convergence. This theory predicts that the amount of PAR absorbed by a canopy is linearly related to its photosynthetic capacity. This, in turn, establishes a theoretical basis for the remote sensing of primary productivity.

The validity of these principles for a particular ecosystem can be tested by examining the relationships between light level and leaf nitrogen and between leaf nitrogen and leaf photosynthetic capacity. Significant correlations between light level and leaf nitrogen within plant canopies have been reported by several authors [*Dejong and Doyle*, 1985; *Hirose and Werger*, 1987b; *Hirose et al.*, 1988; *Hollinger*, 1989, 1996; *Pons and Pearcy*, 1994]. Furthermore, there is also a well-documented relationship between leaf nitrogen and leaf photo-

[1]Centre de Recherche en Biologie Forestière, Université Laval, Sainte-Foy, Quebec, Canada.
[2]Biospheric Sciences Branch, NASA Goddard Space Flight Center, Greenbelt, Maryland.
[3]Now at Lakehead University, Faculty of Forestry, Thunder Bay, Ontario, Canada.
[4]Now at Institute of Biology, Biology Department, Carleton University, Ottawa.
[5]USDA Agricultural Research Service, Remote Sensing Research Laboratory, Beltsville, Maryland.

synthetic capacity [e.g., *Field and Mooney*, 1986; *Hirose et al.*, 1988; *Evans*, 1989; *Walters and Reich*, 1989; *Thompson et al.*, 1992; *Ellsworth and Reich*, 1993; *Mitchell and Hinckley*, 1993; *Reich et al.*, 1994; *Reich and Walters*, 1994; *Tan and Hogan*, 1995; *Brooks et al.*, 1996].

While we might expect boreal forest trees to exhibit an optimized distribution of photosynthetic capacity with respect to light, there are also a number of factors that could cause complications. For example, shoots often contain foliage of different age classes, the physiological characteristics of foliage change over the growing season [e.g., *Abidine et al.*, 1995; *Abrams and Mostoller*, 1995], photosynthesis tends to saturate at lower light levels than typically found at the top of the canopy in midsummer, nitrogen is used in processes not directly related to photosynthesis [*Charles-Edwards et al.*, 1987; *Evans*, 1989; *Kull and Jarvis*, 1995], canopy structure can influence environmental factors other than light (e.g., air temperature), and individual plants may differ in exposure to stress or have access to greater resources than other individuals (e.g., plants capable of biological nitrogen fixation).

In this paper, we first test the extent to which a single measurement of percent photosynthetically active radiation (%PAR) within boreal forest canopies taken under overcast conditions is representative of the average PAR conditions on both cloudy and sunny days. We then examine canopy profiles of PAR flux density, leaf nitrogen content per unit leaf area (N_{area}) and leaf photosynthetic capacity (A_{max}) for five forest stands in the BOREAS northern study area in order to test the functional convergence hypothesis for the boreal forest. To better understand variations in N_{area} that are not explained by PAR levels, we examine the relationships of specific leaf area with A_{max}, N_{area}, and photosynthetic nitrogen use efficiency. Furthermore, to demonstrate the consequences of using different assumptions about the vertical distribution of leaf A_{max} within boreal forest canopies to scale leaf A_{max} to the canopy ($A_{can-max}$), we compare the results of a simple scaling technique using two different theoretical vertical distributions of leaf A_{max} and then compare these results with a calculation of $A_{can-max}$ which used our measured distribution of leaf A_{max}. Finally, we examine the relationship between these calculated $A_{can-max}$ values and two common remote sensing vegetation indices.

Materials and Methods
Study Sites

This study was conducted in the northern study area (NSA) of Boreal Ecosystem-Atmosphere Study [see *Sellers et al.*, 1995, for details] between Nelson House and Thompson, Manitoba, Canada (56°N, 99°W). The forests in this region are typical of northern boreal forests, consisting primarily of black spruce (*Picea mariana* (Mill.) B.S.P.) with some jack pine (*Pinus banksiana* Lamb.) and smaller patches of aspen (*Populus tremuloides* Michx.). The landscape of the region consists of a mosaic of low-relief terrain, moderate size hills, and small lakes. The soils are derived predominantly from glacial Lake Agassiz sediments and consist of clays, organic materials, and some sandy deposits. Treed peatlands are common in lowland areas.

Five forest stands were used for this study, i.e., the lowland old black spruce (NSA-OBS), the upland black spruce (NSA-UBS), the old jack pine (NSA-OJP), the young jack pine (NSA-YJP), and the old aspen (NSA-OASP) stands. The NSA-OBS stand was approximately 75 years old, ranged from

9 to 12 m in height and contained between 600 and 900 stems ha^{-1}. It is located on a peatland site with a high water holding capacity and variable drainage. On the better drained microsites, the ground cover was composed of primarily feather moss (*Hylocomium spp.*) and Labrador tea (*Ledum groenlandicum*). The soil is an orthic grey luvisol. The understory was mostly small black spruce plants established by either seed or layering. On the poorly drained microsites the ground cover was primarily *Sphagnum spp.*, the organic layer depth was between 20 and 100 cm, and the soil is classified as a peaty-phase orthic gleysol.

The upland black spruce stand (NSA-UBS) was approximately 90 years old, had 5976 stems ha^{-1}, and averaged 11.6 m in height. The understory was dominated by small black spruce. Ground cover vegetation consisted primarily of *Pleurozium spp.* with some *Hylocomium splendens* and *Ptilium cristacastrensis*.

The young jack pine (NSA-YJP) was between 20 and 25 years old, ranged from 3 to 5 m in height, and contained 23,000 stems ha^{-1}. The overstory was primarily jack pine with a few aspen. In the area where we sampled, the understory was primarily small black spruce (30 to 80 cm tall) with some *Padus nana* and *Alnus crispa*. The groundcover vegetation was *Cladina spp.*, *Vaccinium vitis-idaea*, and *Ledum groenlandicum*. The soil is sand and gravel over a clay of low water holding capacity. The soil is classified as an eluviated and greyed eluviated dystric brunisol. The organic layer ranged from 3 to 25 cm deep.

The NSA-OJP stand was approximately 58 years old, averaged 9 m in height, and contained 1875 to 3100 stems ha^{-1}. It is located on a sandy outwash of very low water holding capacity. The ground cover was primarily lichen (*Cladina spp.*), although there were some wetter spots that contained *Alnus crispa* and *Pleurozium spp.* Generally, there was no vegetation between the ground cover and the overstory canopy. There was a shallow organic layer of less than 5 cm, and the soil is classified as a brunisol.

The NSA-OASP stand was between 70 and 80 years old, ranged from 16 to 20 m in height, and contained approximately 2000 stems ha^{-1}. The understory was comprised primarily of *Alnus crispa* and *Salix spp.*, while the ground cover contained a variety of herbaceous species dominated by *Cornus canadensis*. The soil is a heavy clay.

All measurements were taken during each of the three 1994 intensive field campaigns (IFCs) of BOREAS [see *Sellers et al.*, 1995, for details]. IFC-1 ran from May 24 to June 16, IFC-2 from July 19 to August 8, and IFC-3 from August 30 to September 19.

Measurement of Diurnal Patterns of PAR on Sunny Versus Cloudy Days

To determine how the percentage of the above-canopy photosynthetically active radiation received in the understory (%PAR) differed on cloudy days versus sunny days, diurnal patterns of %PAR were measured in the understories of the NSA-YJP, NSA-OJP, NSA-OASP, and NSA-UBS stands. One PAR quantum sensor (model Li-190SA, Li-Cor Inc., Lincoln, Nebraska) was installed above the forest canopy where it was exposed to the full incoming PAR. This sensor provided a simultaneous 100% incoming PAR measurement for each measurement made under the forest canopy. Five other PAR sensors were placed at randomly selected locations under the forest canopy at about 0.5 m above the ground. All sensors

were connected to a data acquisition system (model CR10, Campbell Scientific Canada Corp., Edmonton, Canada) fitted with a multiplexer. In order to minimize external interference, a differential configuration was used. Readings were taken every 10 s by the sensors, but only 5 min averages were recorded.

Measurement of %PAR and Foliar Nitrogen Profiles

Percent photosynthetically active radiation (%PAR) was measured at five canopy levels, i.e., the top, the middle, and the bottom of the crown, at the top of the understory, and just above the ground cover. Measurements were always taken under overcast conditions, i.e., no direct beam radiation or shadows were present. If the Sun came out during a series of measurements, work was discontinued until overcast conditions returned. The within-canopy PAR measurements were made with a Li-190SA quantum PAR sensor attached to a pole. The canopy level measurements for the mature stands were taken from scaffolding towers. The scaffolding towers were moved between IFCs. A second sensor was installed on another pole which was mounted on the canopy access tower such that the sensor extended over the top of the forest canopy. This sensor provided the 100% PAR reference measurement. Both the above-canopy and the below-canopy sensors were connected to a data acquisition system (model CR10, Campbell Scientific Canada Corp., Edmonton, Canada).

The within-stand measurements were taken at five randomly selected points at each of the five levels. The branch or ground cover located directly below the point of the PAR measurements was then harvested for nitrogen determination. For the measurement of the groundcover, 1×1 m plots were used. PAR measurements began at ground level and proceeded upward. The CR10 was programed to take input readings every 5 s and to output 1 min averages. The minimum period for a PAR measurement was 2 min. The total height of the forest canopy and the height of the sensor for each PAR measurement were recorded.

The hemisurface leaf areas of the broadleaf species were measured with an AgVision root and leaf area imaging measurement system [Decagon Devices Inc., Pullman, Washington]. The hemisurface leaf areas of coniferous samples were determined using the volume displacement method [Brand, 1987]. The shape factor used for the calculation of the hemisurface area was determined to be 4.00 for black spruce and 4.59 for jack pine.

The samples from the profiles were oven-dried at 68°C for 48 hours, ground, and then stored in sealed plastic bags until microkjeldahl nitrogen analyses were begun. The samples were oven-dried for an additional two hours just prior to beginning the nitrogen analyses. For conifers, current-year foliage was analyzed separately from older foliage. Nitrogen concentration was expressed on the basis of both dry-mass and hemisurface area.

Measurement of Photosynthetic Capacity

The light-saturated rates of net photosynthesis of branches sampled from different canopy levels were measured under controlled environmental conditions in the laboratory at 20° ± 0.5°C air temperature, 0.6 ± 0.2 kPa water vapor pressure deficit, 360 ± 10 μmol mol^{-1} CO$_2$ concentration, and 1100 μmol m^{-2} s^{-1} PAR. Henceforth, we refer to this as photosynthetic capacity (A_{max}).

Tests indicated that reliable measurements could be obtained for up to 14 hours after harvesting the branches for pine

and spruce and for up to 10 hours after harvest for aspen (see Dang et al. [1997] for details about the testing procedures). Samples were harvested from three levels in each stand. For the NSA-OBS, NSA-UBS, and NSA-OJP stands, the (1) top, (2) middle, and (3) bottom of the canopy were sampled. For the NSA-OASP and NSA-YJP stands, the (1) top and (2) middle of the crown were sampled in addition to (3) the understory. Alnus crispa was the understory vegetation sampled in the NSA-OASP stand and the small 30–80 cm tall black spruce was the understory vegetation sampled in the NSA-YJP stand. The samples from large trees were harvested using a 12-gage shotgun. Branches from small trees or understory vegetation were cut using extendible pruning shears or hand clippers. The samples were taken from five individual plants from each canopy level between 0500 and 0700. Immediately after harvesting, the branches were recut under water, and the cut surface was kept submerged during the 30–50 min trip to the laboratory and up to the time of measurement. The foliage was kept above the water surface by using a styrofoam support structure inside a cooler filled with water.

The gas exchange rates of carbon dioxide and water vapor were measured using an open gas exchange system, which consisted of a LiCor-6262 infrared gas analyzer, two leaf cuvettes, and an environmental control system [Yue et al., 1992]. Eight branches were measured from each canopy layer, but each sample was measured only once. To avoid possible confounding effects due to the time of measurement, a pair of samples were measured first from the upper canopy, then the middle, and finally the bottom. The sequence was repeated until all branches were measured. For conifers, foliage of all age classes was measured together on a single branch. The light passed through an 8 cm thick water-filled filter before reaching the foliage to avoid excess heating inside the cuvette. To keep an adequate supply of water to the branch during the measurement, the cut end of the stem was connected to a column of water running through a plastic tube. The environmental conditions inside the leaf cuvettes (including CO$_2$ concentration and water vapor partial pressure) were monitored continuously using an automated data acquisition system which included a LiCor-6262 infrared gas analyzer; pressure, temperature, and PAR sensors; an MT-1000 board (Measurement Technology Inc., Stoughton, Massachusetts); and an IBM 286 microcomputer. A measurement was made when the exchange rates of CO$_2$ and H$_2$O became stable and only the steady state reading was used for the calculation of photosynthesis.

Leaf area and nitrogen concentration of the foliage were determined as described above. The rate of photosynthesis was calculated according to von Caemmerer and Farquhar [1981]. Photosynthesis and foliar nitrogen concentration were expressed on a hemisurface surface basis as is the convention for BOREAS. Photosynthetic nitrogen use efficiency (NUE) was calculated as the ratio of photosynthetic capacity to nitrogen concentration.

Data Analyses

The extinction of PAR with depth in the forest canopy under diffuse light conditions was approximated by Beer's law:

$$\ln (I_z/I_0) = -k_D D \qquad (1)$$

where I_z and I_0 are the irradiance for PAR above and within the canopy, respectively; k_D is the extinction coefficient with
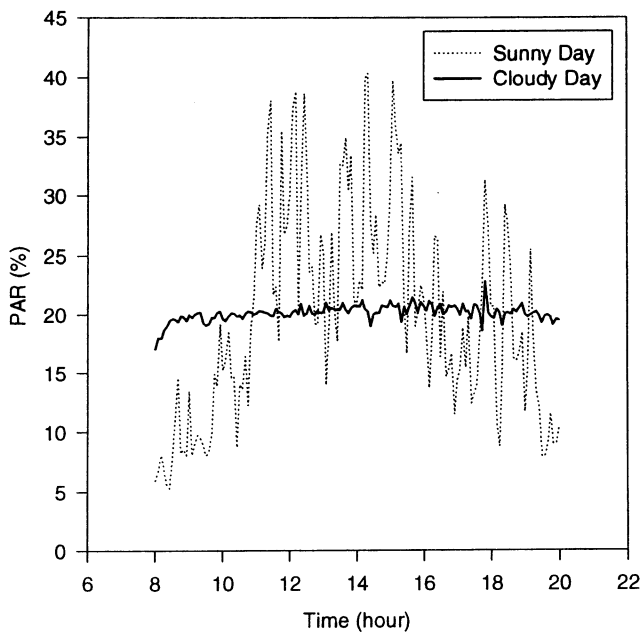
Figure 1. Diurnal measurements of photosynthetically active radiation (PAR) under the canopy of the old aspen stand on a cloudy day (June 12) and a sunny day (June 8) in 1994. PAR values are expressed as a percentage of the PAR above the forest canopy (%PAR); $n = 5$.

canopy depth; and D is the depth from the top of the canopy. We used a slightly modified version of (1) in our analysis since we wanted to express I_z/I_0 as a percentage.

$$\ln (\%PAR) = \ln (100) - k_D D \qquad (2)$$

For the analysis of the relationship between foliar nitrogen per unit leaf area (N_{area}) and %PAR, we used

$$N_{area} = a + b \log (\%PAR) \qquad (3)$$

where a and b are the intercept and slope of the regression, respectively. Although a linear model would also have fit the data, the log transformation of %PAR increased the goodness of fit. Note that the term IPAR, commonly used in remote sensing for the fraction of PAR intercepted by a canopy, is equal to $(100 - \%PAR)/100$. For our analysis we used %PAR because, unlike IPAR, it does not become mathematically undefined at the top of the canopy when used in (3).

For analyzing the relationship between photosynthetic capacity expressed on the basis of hemisurface leaf area (A_{max}, $\mu mol\ m^{-2}\ s^{-1}$) and nitrogen per unit hemisurface leaf area (N_{area}), we used

$$A_{max} = c + d\ N_{area} \qquad (4)$$

where c and d are the intercept and slope of the regression, respectively.

Differences in all of the above relationships among different stands, species, foliage age classes, and IFCs were examined by comparing regression parameters using the maximum likelihood statistic method [Neter et al., 1990; Sarndal et al., 1992]. The distributions of residuals for all the regressions were examined as described by Draper and Smith [1981]. Ground cover data were not used in testing the effect of foliage age.

With D set to zero and %PAR to 100, (2), (3), and (4) were

used to calculate A_{max} at the top of the canopy (A_{max0}); that is, $A_{max0} = c + ad + 2bd$. Relative photosynthetic capacity ($\%A_{max0}$) at any D or %PAR is expressed as a percentage of A_{max0}. We calculated the parameters a, b, c, and d from IFC-2 and IFC-3 data only.

Leaf Area Index, Normalized Difference Vegetation Index (NDVI), and Simple Ratio (SR)

Overstory leaf area indices of the five stands were obtained from BOREAS terrestrial ecology team 6 (TE-6) led by S. T. Gower (University of Wisconsin) as accessed through the BOREAS Information System (BORIS). Leaf areas were calculated by TE-6 from allometric relationships developed from trees harvested from each site. Refer to the BORIS documentation for TE-6 for further information.

The normalized difference vegetation index (NDVI) and the simple ratio (SR) were calculated as

$$NDVI = (\rho_{NIR} - \rho_{RED})/(\rho_{NIR} + \rho_{RED}) \qquad (5)$$

$$SR = (\rho_{NIR}/\rho_{RED}) \qquad (6)$$

where ρ_{NIR} and ρ_{RED} are reflectances in the near-infrared and red wave bands, respectively.

Canopy reflectances were measured by a NASA helicopter equipped with a Barnes multiband modular radiometer on a pointable mount [Walthall et al., 1996]. Visible and near-infrared radiances were obtained from 300 m above the canopy using 15° field-of-view lenses. Sensor voltages were converted to at-sensor radiances using procedures detailed by Markham et al. [1988]. The at-sensor radiances were then atmospherically corrected and normalized to provide at-surface reflectances. Optical depth measurements from the surface-based Sun photometer network at each study area were used to provide data necessary for irradiance and atmospheric corrections (see Loechel et al. [this issue] for further details). NDVI and SR were calculated from the mean at-surface reflectances for each site for IFC-2. The reflectance data used for this analysis are a subset of the full data set of these sites.

Results

Diurnal Patterns of %PAR on Sunny Versus Cloudy Days

Percent PAR in the understories were very stable under cloudy conditions but fluctuated 20% or more over short time periods under sunny conditions (Figure 1). Despite this large variability in %PAR over time on sunny days, differences in the average diurnal %PAR under cloudy versus sunny conditions were not significant ($p > 0.05$, $n = 5$) for any of the four stands studied (Figure 2). There was a tendency for the more open stands, NSA-YJP and NSA-OJP, to have somewhat higher %PAR values on cloudy days. The differences, however, were less than 8%. Thus a short-term measurement of %PAR within these canopies under overcast conditions provides a fairly representative measure of the integrated %PAR environment at a given time of the year.

Canopy Depth Versus %PAR

Percent PAR decreased significantly ($p < 0.0002$) with increasing depth from the top of the canopy in all five stands measured and equation (2) yielded correlation coefficients (r) ranging from 0.73 to 0.92 (Figure 3). The upland black spruce stand (NSA-UBS) had a significantly higher extinction coefficient, k_D, than the other three stands, while k_D for NSA-OJP

was significantly lower ($p < 0.04$, Figure 4). There were no significant differences in k_D between the NSA-YJP, NSA-OBS, and NSA-OASP stands ($p > 0.05$, Figure 4). The model for the NSA-YJP, NSA-OBS, and NSA-OASP stands combined was not significantly different from the model for all five stands combined ($p = 0.9801$). For all stands combined, k_D and r were 0.160 and 0.78, respectively.

The minimum %PAR level measured just above the ground cover of these five stands was correlated strongly with NDVI ($r = 0.91$, $p < 0.0001$; Figure 5a). The simple ratio index was less strongly correlated with minimum %PAR ($r = 0.76$, $p < 0.0001$; Figure 5b).

%PAR Versus Nitrogen

Nitrogen per unit leaf area (N_{area}) decreased significantly with decreasing %PAR for each of the five individual stands, for all conifer stands combined ($r = 0.52$), and for all stands combined ($r = 0.46$) (Table 1, Figure 6). However, there were significant differences in the %PAR $-$ N_{area} relationship between aspen and conifers ($p < 0.01$, Table 1). The N_{area} of all conifer stands was significantly more sensitive to %PAR than that of the NSA-OASP stand (slope 0.60 versus 0.30, Table 1). The N_{area} of the NSA-OBS stand was also significantly more sensitive than that of the NSA-UBS stand (slope 0.60 versus 0.36, $p = 0.02$), but there were no significant differences between the NSA-YJP and the NSA-OJP stands, or between black spruce and jack pine stands ($p > 0.05$).

There were no significant differences in the %PAR $-$ N_{area} relationship between different IFCs for all stands combined and all conifer stands combined ($p > 0.40$). For the NSA-OASP stand, however, there was a significant difference in this
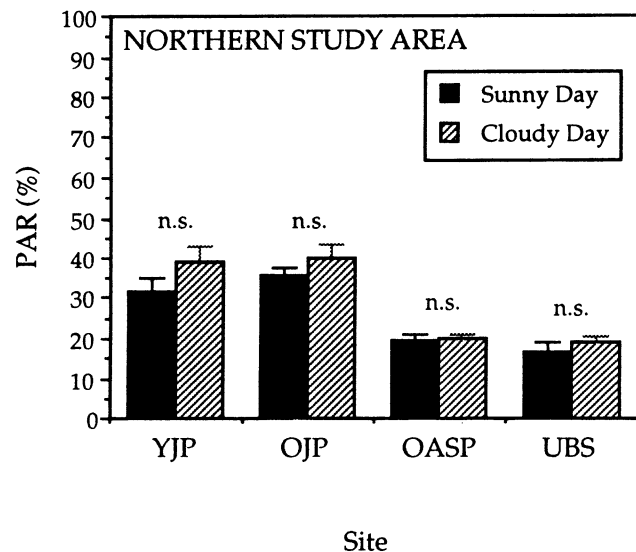

Figure 3. Percent PAR in relation to depth from the top of the forest canopy for the (a) NSA-YJP, (b) NSA-OJP, (c) lowland old black spruce (NSA-OBS), (d) NSA-UBS, and (e) NSA-OASP stands in the BOREAS NSA. Stand codes are as defined in Figure 2. Data are from all three intensive field campaigns (IFCs).

relationship between IFC-1 and the other two IFCs ($p < 0.0058$). Because of the higher N_{area} of the understory alder just after budbreak in IFC-1 (outlying open circles in Figure 6c), N_{area} actually increased with decreasing %PAR for the

Figure 2. Daily average %PAR on a sunny and a cloudy day under the canopy of the young jack pine (NSA-YJP), old jack pine (NSA-OJP), old aspen (NSA-OASP), and upland black spruce (NSA-UBS) stands. Values are expressed as the percentage of PAR relative to that measured above the forest canopy. Within the same stand, the mean %PAR on the sunny day was not significantly (n.s.) different from that on the cloudy day ($p > 0.05$, $n = 5$). Sunny day and cloudy day measurements were taken, respectively, on May 25 and June 3 for NSA-YJP, June 7 and May 29 for NSA-OJP, June 8 and June 12 for NSA-OASP, and June 2 and May 31 for NSA-UBS.
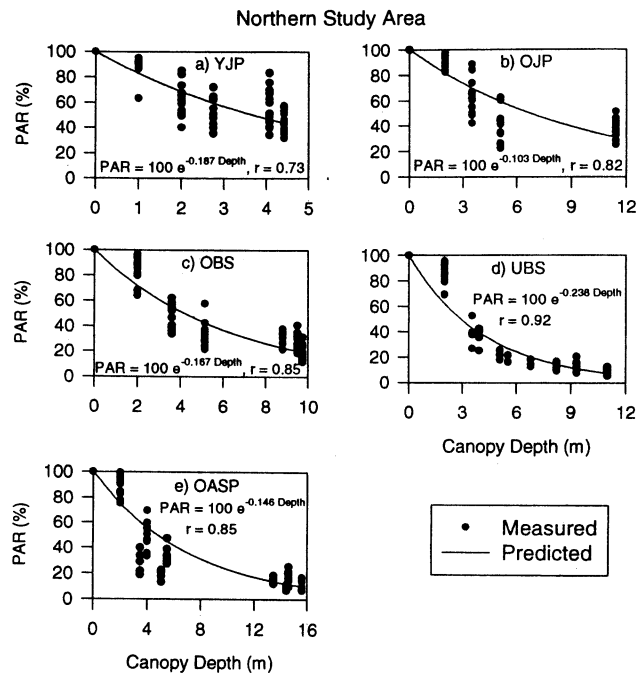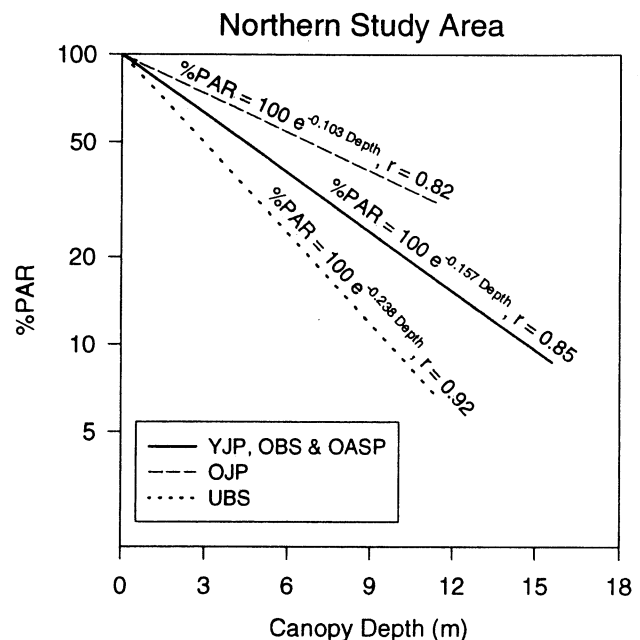

Figure 4. Extinction of %PAR with canopy depth for the NSA-OJP and NSA-UBS stands and the NSA-YJP, NSA-OBS, and NSA-OASP stands combined. Stand codes are as defined in Figures 2 and 3.
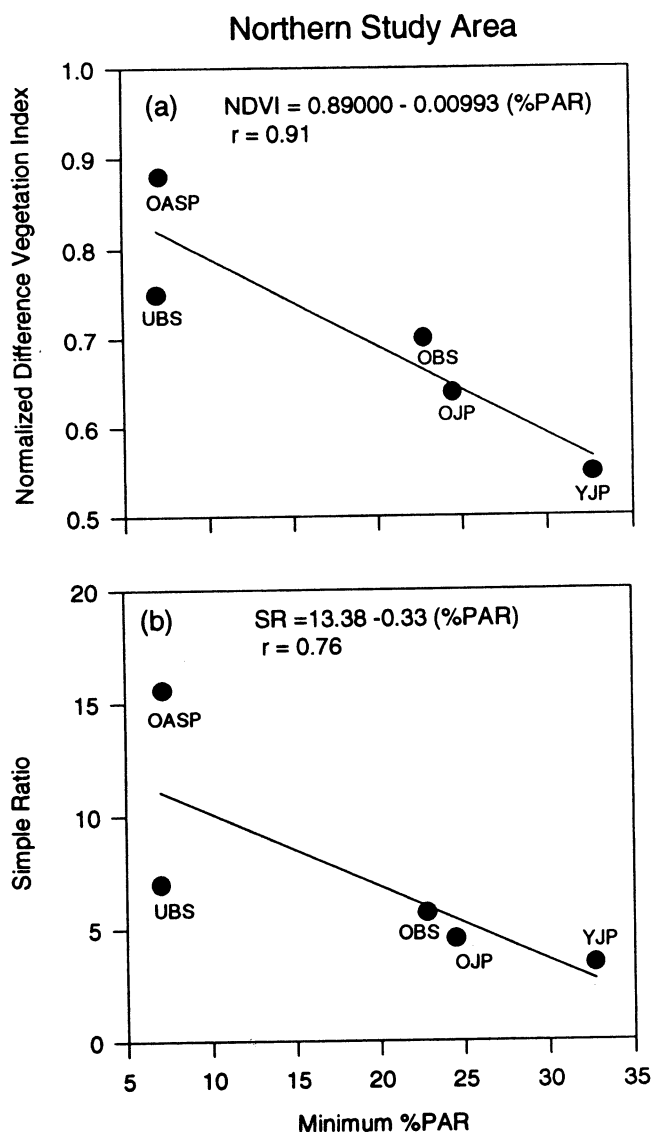
Northern Study Area

Figure 5. (a) Normalized difference vegetation index (NDVI) and (b) simple ratio measured from the NASA helicopter during IFC-2 in relation to the minimum %PAR (n = 5) measured in the understory of the NSA-YJP, NSA-OJP, NSA-OBS, NSA-UBS, and NSA-OASP stands. Stand codes are as defined in Figures 2 and 3.

aspen stand in IFC-1, while it decreased with decreasing %PAR in IFC-2 and IFC-3. When alder was removed from the analysis, the seasonal variation in the %PAR − N_{area} relationship for the NSA-OASP became insignificant (p = 0.6544), and the %PAR − N_{area} regression was improved for the aspen stand and for all stands combined (Table 1). Nevertheless, N_{area} of alder did follow a different seasonal pattern than aspen. Average N_{area} for alder decreased from 1.84, to 1.59, and to 1.03 g m^{-2} for IFC-1, IFC-2, and IFC-3, respectively, while it went from 1.44, to 1.58, and to 1.23 g m^{-2} over the same period for aspen.

Foliage age class did not significantly affect the %PAR − N_{area} relationship for conifers (p = 0.8786).

Nitrogen Versus Photosynthesis

Photosynthetic capacity (A_{max}; μmol m^{-2} s^{-1}) decreased significantly with decreasing foliar nitrogen per unit leaf area

(N_{area}) for all stands combined, all conifer stands combined, and for the aspen stand alone (Figure 7, Table 2). However, the model for all stands combined underestimated A_{max} for the aspen stand and overestimated it for the conifers (Figure 7a). Additionally, there were significant interactions between species and IFCs. Jack pine had a significant negative relationship between N_{area} and A_{max} in IFC-1 (Figure 8), while the relationship was positive in IFC-2 and IFC-3 (data not shown). This resulted in an insignificant relationship between N_{area} and A_{max} when jack pine data from all three IFCs were pooled together (Table 2). The N_{area} − A_{max} relationship was dramatically improved when IFC-1 data were eliminated from the analysis for all stands (r = 0.51), all conifer stands (r = 0.60), and jack pine stands (r = 0.56) (Table 2). For the black spruce and aspen stands, on the other hand, removing IFC-1 data had little effect (Table 2).

The slope of the N_{area} − A_{max} regression was significantly greater for aspen than for conifers (p ≤ 0.0002, Table 2). However, there were no significant differences between the slopes of jack pine and the black spruce (p > 0.11) when the IFC-1 data were removed (Table 2). There were also no significant differences between the NSA-YJP and NSA-OJP stands (p > 0.76), or between NSA-OBS and NSA-UBS stands (p > 0.65). In contrast to the %PAR − N_{area} relationship for which N_{area} for alder in IFC-1 was similar to or higher than that for aspen at the same %PAR (Figure 6c), all of the N_{area} − A_{max} data for alder fell along the same line as the aspen data (Figure 7c), and the regression model gave a better fit when alder was included (Table 2). Stomatal conductance was very strongly correlated (r = 0.96, p < 0.0001) with A_{max} for all species, canopy positions, and IFCs combined together (Figure 9).

Relative Photosynthetic Capacity (%A_{max0}) Versus Canopy Depth, %N_{max0}, and %PAR

Relative nitrogen content (%N_{max0}) is defined as the nitrogen concentration (N_{area}) at a given canopy level expressed as a percentage of the nitrogen concentration in the upper canopy (N_{max0}). Similarly, relative photosynthetic capacity (%A_{max0})

Table 1. Regression Analysis of the Relationship Between %PAR and Nitrogen Content per Unit Leaf Area (N_{area}; g m^{-2})

Stand	a	b	r	Prob
All	0.55	0.50	0.46	0.0001
All (−alder)	0.46	0.55	0.50	0.0001
NSA-OASP	0.98	0.30	0.41	0.0012
NSA-OASP (−alder)	0.84	0.36	0.58	0.0001
NSA-OASP (−IFC-1)	0.81	0.40	0.54	0.0001
All conifers	0.36	0.60	0.52	0.0002
NSA-OBS	0.29	0.60	0.57	0.0001
NSA-UBS	0.64	0.36	0.54	0.0001
Both black spruce	0.58	0.42	0.50	0.0001
NSA-OJP	0.69	0.53	0.41	0.0003
NSA-YJP	0.71	0.44	0.28	0.0001
Both jack pine	0.76	0.45	0.31	0.0001

Using the model, N_{area} = a + b log (%PAR). Note that "−alder" and "−IFC-1" indicate the elimination of alder and IFC-1 data, respectively; r, correlation coefficient; prob, probability level; NSA-OASP, old aspen; NSA-OBS, lowland old black spruce; NSA-UBS, upland black spruce; NSA-OJP, old jack pine; NSA-YJP, young jack pine in the northern study area (NSA) of BOREAS.

is defined as the photosynthetic capacity (A_{max}) at a given canopy level expressed as a percentage of the upper canopy photosynthetic capacity (A_{max0}). There was a one-to-one relationship between the $\%N_{max0}$ and the $\%A_{max0}$ for the NSA-OASP stand (Figure 10a); for example, a 50% decrease in $\%N_{max0}$ resulted in a 50% decrease in $\%A_{max0}$. For the coni-

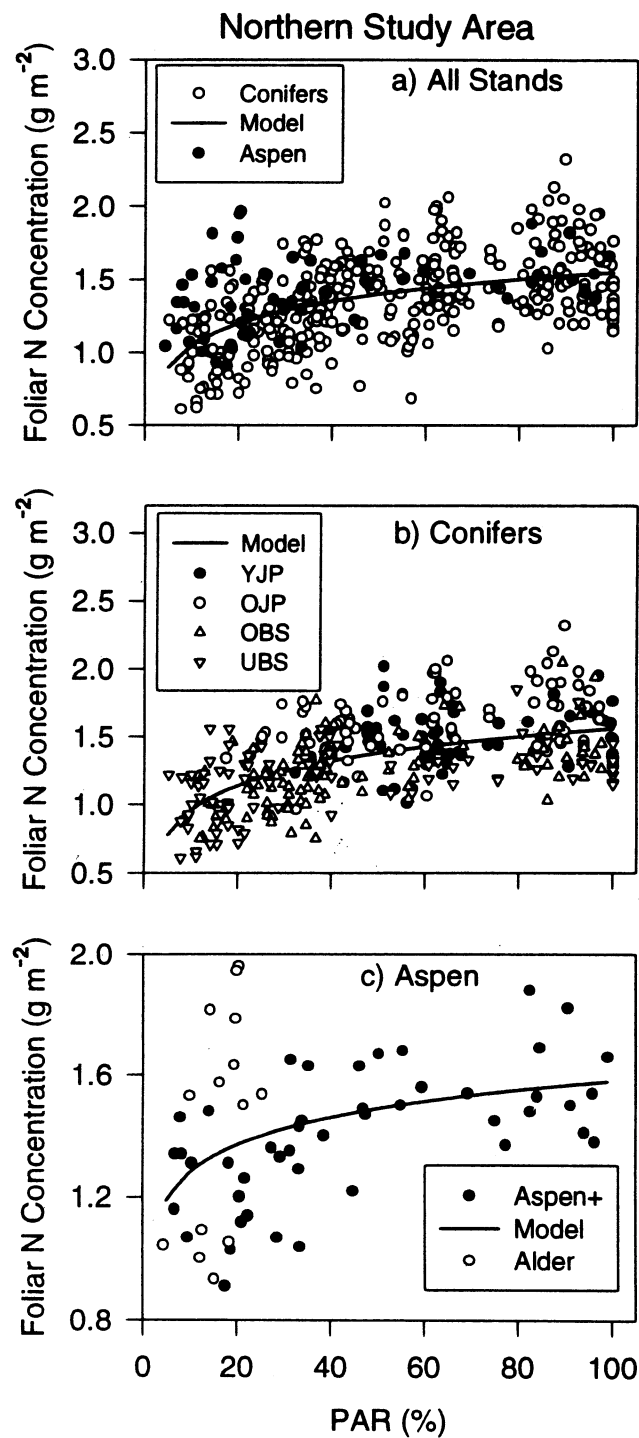**Figure 6.** Foliar nitrogen per unit leaf area (N_{area}) in relation to %PAR for (a) all stands, (b) conifer stands only, and (c) the aspen stand alone. Refer to Table 1 for models and associated parameters. "Aspen+" indicates aspen and the ground cover of the aspen stand. Data are from all three IFCs.
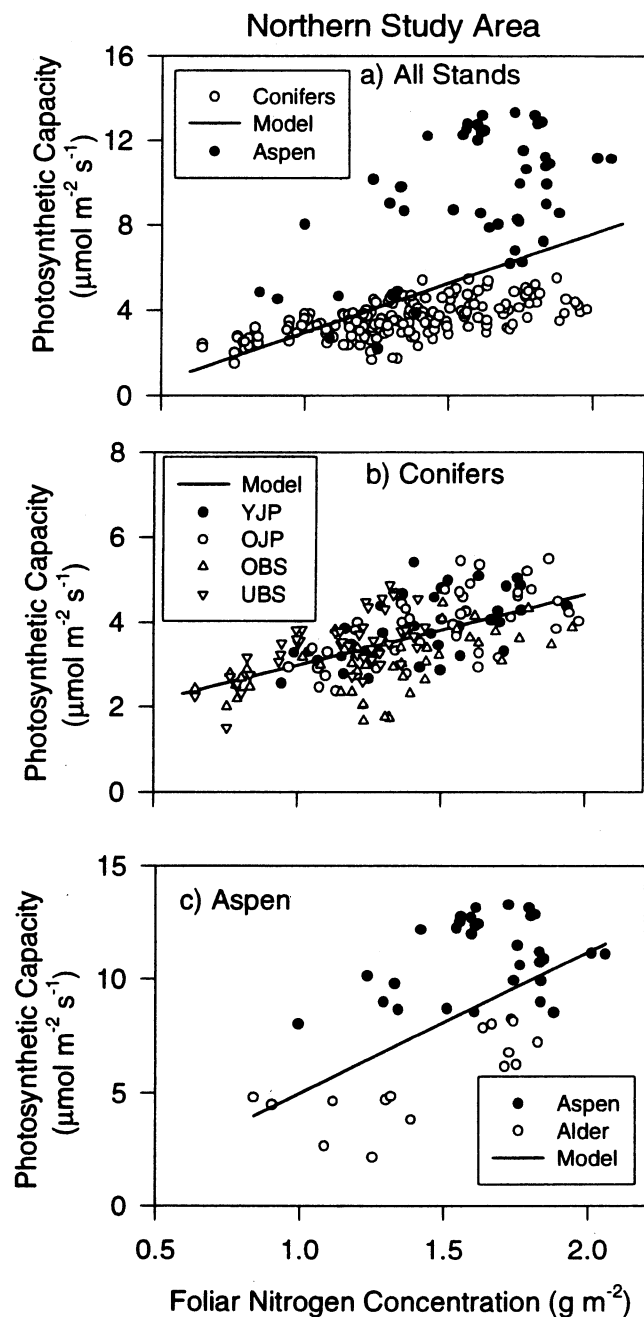

Figure 7. Photosynthetic capacity (A_{max}) in relation to foliar nitrogen per unit hemisurface leaf area (N_{area}) for (a) all stands, (b) conifer stands only, and (c) the aspen stand alone. Only data from IFC-2 and IFC-3 are presented. Refer to Table 2 for models and associated parameters. Stand codes are as defined in Figures 2 and 3. Data are from three canopy levels of the overstory species for NSA-OJP, NSA-UBS, and NSA-OBS and from the top and middle levels of the crown plus the understory for the NSA-YJP and NSA-OASP. The understories of the NSA-OASP and NSA-YJP were alder and black spruce, respectively.

fers, however, $\%N_{max0}$ decreased faster than $\%A_{max0}$ (Figure 10a).

When $\%A_{max0}$ was compared to %PAR, all five stands were found to scale their respective $\%A_{max0}$ values to %PAR in a similar manner (Figure 10b). Thus stands with a higher PAR

Table 2. Regression Analysis Between Foliar Nitrogen per Unit Leaf Area (N_{area}, g m^{-2}) and Photosynthetic Capacity (A_{max}, μmol m^{-2} s^{-1})

Stand	Data From all IFCs				Data From IFC-2 and IFC-3 Only			
	c	d	r	Prob	c	d	r	Prob
All	−0.108	3.369	0.37	0.0001	−1.640	4.606	0.51	0.0001
All (−alder)	0.775	2.617	0.30	0.0001	−1.667	4.589	0.49	0.0001
Aspen	1.727	5.183	0.52	0.0003	0.058	5.826	0.54	0.0001
Aspen (−alder)	7.218	2.302	0.31	0.0302	7.451	2.157	0.31	0.0803
Conifers	1.977	0.995	0.34	0.0230	1.290	1.683	0.60	0.0001
Jack pine	4.193	−0.292	0.09	0.2856	1.161	1.874	0.56	0.0003
Black spruce	0.976	1.657	0.51	0.0023	1.778	1.182	0.45	0.0002

Using the model, $A_{max} = c + d \cdot N_{area}$. Note that "−alder" indicates the elimination of alder data from the analysis. Other definitions as in Table 1.

extinction coefficient also had a faster rate of decline in $\%A_{max0}$ (Figure 11). However, %PAR declined much more rapidly than did $\%A_{max0}$ (Figure 10b); that is, $\%A_{max0}$ did not scale proportionally to %PAR. For example, at 40% PAR the $\%A_{max0}$ values were 90% for the NSA-OASP, 92% for NSA-OJP, 93% for NSA-YJP, 90% for NSA-OBS, and 93% for NSA-UBS.

Specific Leaf Area Versus A_{max}, N_{area}, and Nitrogen Use Efficiency

A_{max} was significantly correlated to specific leaf area (SLA) only when all species were combined together ($r = 0.76, p < 0.0001$, Figure 12a). Nitrogen per unit leaf area (N_{area}) was negatively correlated to SLA for the conifers ($r = 0.60, p < 0.0001$), the aspen ($r = 0.74, p < 0.0001$), and the alder and aspen together ($r = 0.45, p < 0.0001$) (Figure 12b). However, there was no correlation between N_{area} and SLA when all species were combined together (Figure 12b).

Photosynthetic nitrogen use efficiency (NUE) (μmol CO_2 s^{-1} g^{-1} N) increased with increasing specific leaf area (SLA) (cm^2 g^{-1}) when all species were combined together ($r = 0.83$, $p < 0.0001$, Figure 12c). However, this was primarily due to the large differences between conifers and broadleaf species. NUE was also significantly correlated to SLA for the conifers ($r = 0.41, p < 0.0001$), the aspen ($r = 0.50, p < 0.0003$), and the alder ($r = 0.64, p < 0.0012$). NUE was less sensitive to SLA above 150 cm^2 g^{-1} (Figure 12c).

Discussion

The %PAR levels measured under diffuse light conditions in the understory were very stable over the course of a day (Figure 1). Furthermore, they did not differ significantly from the mean %PAR measured on sunny days for any of the five stands (Figure 2). *Messier and Puttonen* [1995] showed similar results in a more detailed study of the light environment in a *Pinus sylvestris* stand in Finland. They concluded that PAR measurements taken under diffuse light conditions provide the basis for
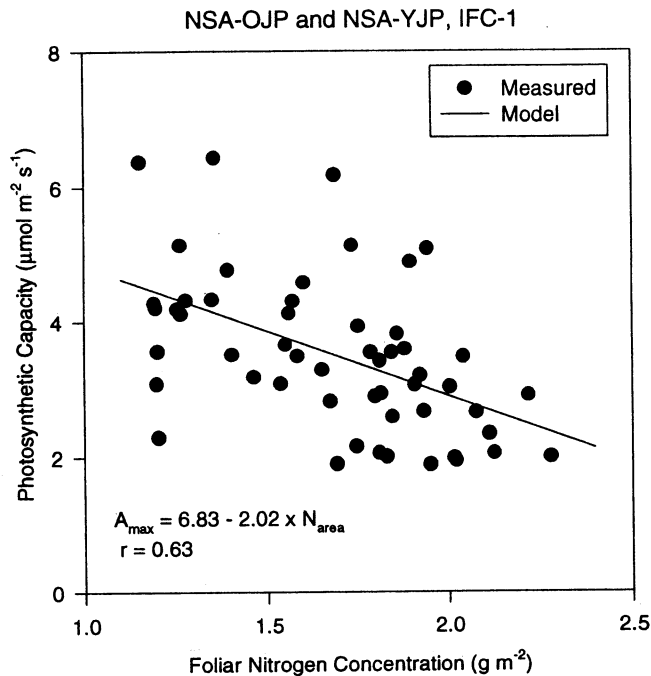

Figure 8. Photosynthetic capacity (A_{max}) in relation to foliar nitrogen per unit hemisurface leaf area (N_{area}) for the NSA-YJP and NSA-OJP stands in the BOREAS NSA in IFC-1.
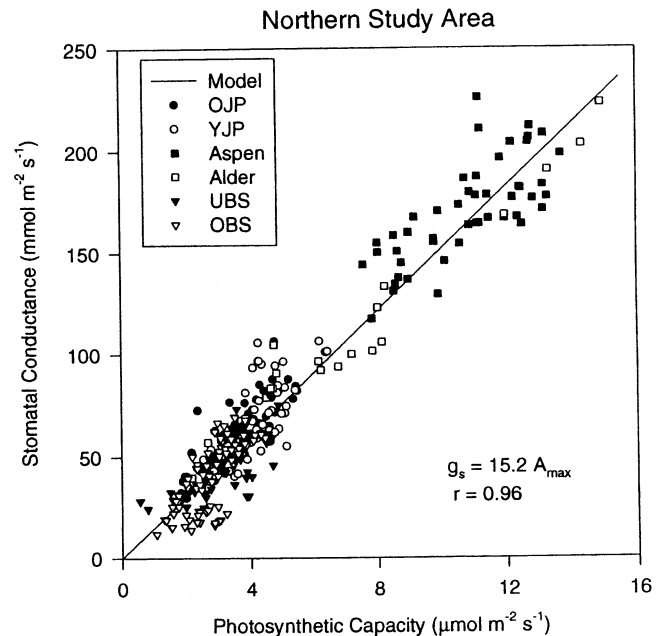
Figure 9. Stomatal conductance to water vapor in relation to photosynthetic capacity (A_{max}) for the NSA-OJP, NSA-YJP, NSA-UBS, NSA-OBS, and NSA-OASP stands. Data are from all three IFCs. See Figure 7 for additional details.
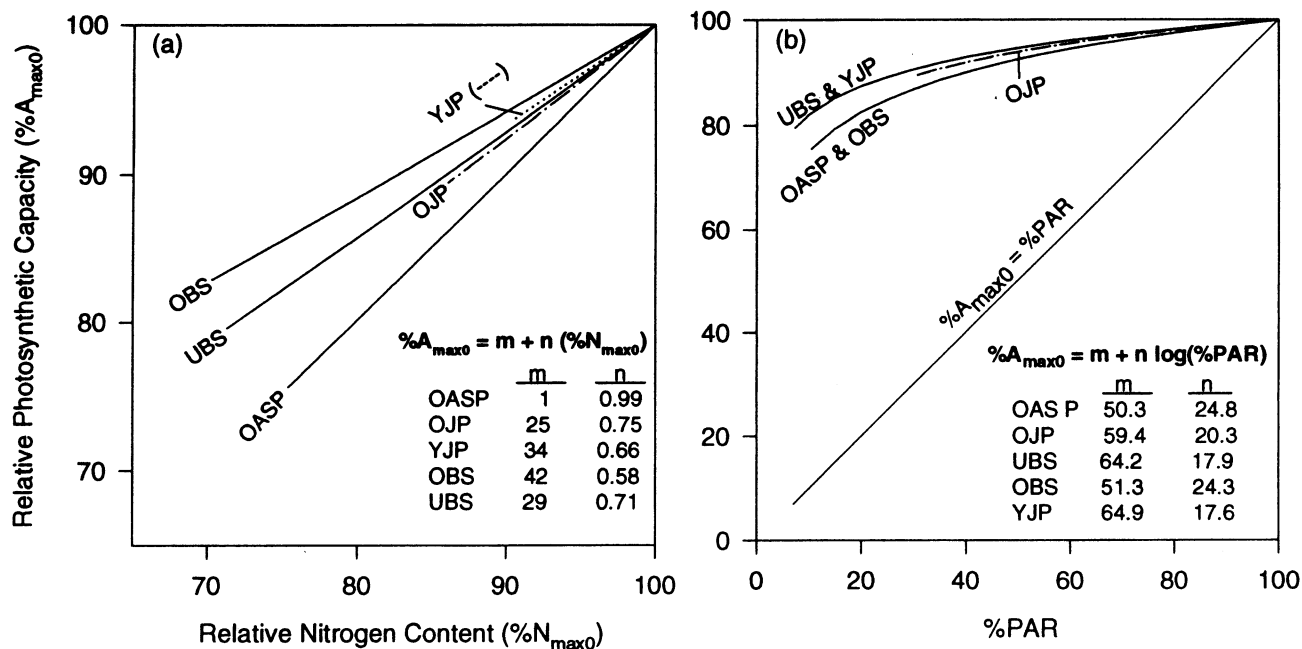
Northern Study Area

Figure 10. Relative leaf photosynthetic capacity, i.e., photosynthetic capacity at a given canopy level expressed as a percentage of that in the upper canopy ($\%A_{max0}$) in relation to (a) relative nitrogen concentration, $\%N_{max0}$, and (b) %PAR. Parameters are derived from IFC-2 and IFC-3 data only.

a quick and efficient means of characterizing the light environment within forest stands. However, diffuse light is better capable of penetrating the forest canopy and illuminating foliage from multiple angles [*Landsberg*, 1986]. This effect was some-

Figure 11. Rate of decrease in $\%A_{max0}$ with increasing canopy depth (% m^{-1}) in relation to the PAR extinction coefficient with regard to canopy depth (k_D). Stand codes as defined in Figures 2 and 3.

what evident in the two least dense of our five stands, i.e., the NSA-YJP and NSA-OJP stands. For these two stands, cloudy day %PAR values were 4%–7% higher than under sunny conditions. These differences, however, were not significant.

Beer's law describes the attenuation of light with depth through a homogeneous canopy with randomly dispersed foliage elements. Despite the nonrandom distribution of foliage in boreal forest stands [*Chen*, 1996], our data show that the Beer's exponential light interception model can still provide a reasonable estimate of the PAR environment under diffuse light conditions in boreal forest canopies. Correlation coefficients between %PAR and canopy depth ranged from 0.73 to 0.92. More detailed dispersed foliage radiative transfer schemes have been developed [e.g., *Norman*, 1979; *Verhoef*, 1984; *Jupp and Strahler*, 1991; *Otterman and Brakke*, 1991]. Nevertheless, the Beer's law formulation is still of interest for large-scale modeling applications because of its simplicity and ease with which integration to whole canopy physiological properties can be accomplished. On the other hand, *Chen and Black* [1991] and *Smith et al.* [1993] have demonstrated that branch architecture can be quite important in modeling radiative transfer within conifer canopies such as Douglas fir (*Pseudotsuga menziesii*). They proposed using a clumping factor that modifies the extinction coefficient in order to take account of branch architecture.

The functional convergence hypothesis implies a general linear relationship between PAR availability and foliar nitrogen. A general relationship did exist between %PAR and nitrogen for our data, but it tended to be weak ($r = 0.46$, $p < 0.0001$, Table 1). Furthermore, although the relationship tended to be curvilinear at low %PAR values, it was basically linear at higher %PAR values (Figure 6). The plants measured in this study included a wide variety of species and life forms growing on the full range of site conditions prevalent on north-
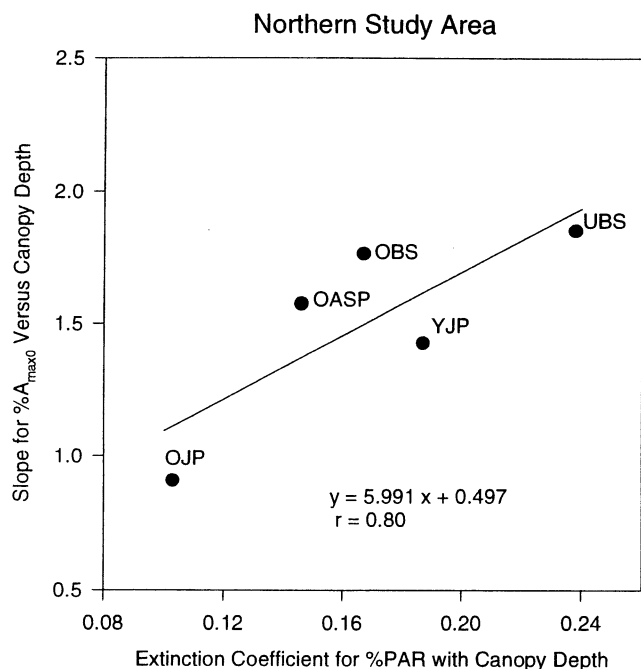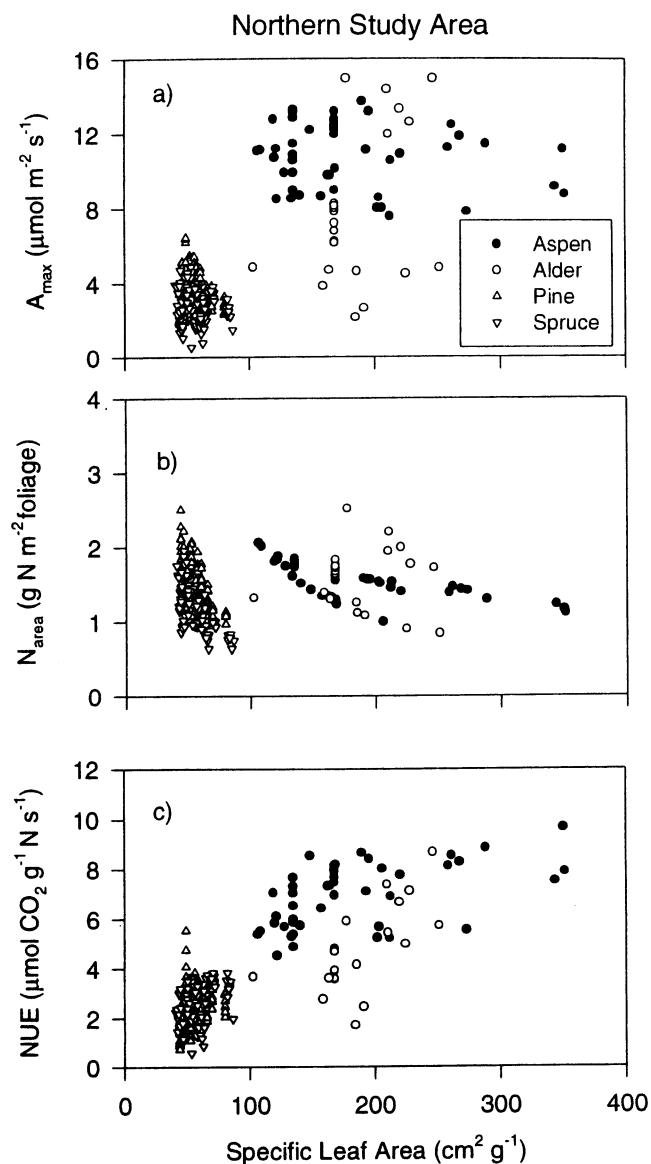
Northern Study Area

Figure 12. (a) Photosynthetic capacity (A_{max}), (b) foliar nitrogen content per unit leaf area (N_{area}), and (c) photosynthetic nitrogen use efficiency (NUE) in relation to specific leaf area. Data are from all three IFCs.

ern boreal forest sites in Canada. The plants from which the %PAR versus nitrogen relationship was developed included ground cover, understory, and overstory species; potentially nitrogen fixing and nonnitrogen fixing species; bryophytes, gymnosperms, and angiosperms. Site conditions ranged from wetland forest sites to dry sandy uplands. Although these various plants were exposed to different environmental stresses and resource limitations, their leaf nitrogen concentrations were all reasonably constrained around the same line with respect to %PAR (Table 1). A more detailed, long-term record of the radiation environment to which the foliage was exposed would likely have improved the correlation coefficients. As well, a consideration of the differences between species in the amount of nitrogen that is not part of photosynthetic function might also have improved the correlation [*Kull and Jarvis*, 1995]. Our data indicate that there are indeed differences in the proportion of leaf nitrogen allocated to photosynthetic

versus nonphotosynthetic functions between leaves at different positions in the canopy and between aspen and conifers (Figures 10a and 12a). The average fraction of PAR absorbed per unit hemisurface area of foliage was similar among the three principal species, averaging 0.79, 0.82, and 0.83 for aspen, jack pine, and black spruce, respectively [*Middleton et al.*, this issue]. Consequently, it is unlikely that the unexplained variability in the %PAR versus N_{area} correlations would have decreased dramatically had we used absorbed PAR instead of incoming PAR.

While there was a general tendency for boreal forest plants to allocate leaf nitrogen based on the availability of PAR in a similar manner (Figure 6, Table 1), our data also revealed an exception to this rule. *Alnus crispa* in the understory of the NSA-OASP stand, a species with the potential to fix atmospheric nitrogen, showed a different relationship between %PAR and foliar nitrogen shortly after budbreak (i.e., IFC-1) than did the other species (Figure 6c, Table 1). Interestingly, during IFC-2 and IFC-3, the relationship between %PAR and nitrogen for alder fell within the general range of points for the aspen stand, although alder does appear to have a steeper slope than aspen. Nevertheless, except for the period shortly after budbreak, even a species with the potential to fix atmospheric nitrogen allocated its foliar nitrogen based on light availability in a manner similar to the other species.

The functional convergence hypothesis also states that there should be a general relationship between nitrogen concentration (N_{area}) and photosynthetic capacity (A_{max}) among species due to the fact that the majority of foliar nitrogen is associated with photosynthesis [*Field*, 1991]. A linear relationship between nitrogen concentration on an area or dry weight basis and A_{max} has been reported for a number of different species [e.g., *Field et al.*, 1983; *Field and Mooney*, 1983, 1986; *DeJong and Doyle*, 1985; *Seemann et al.*, 1987; *Evans*, 1989; *Hirose et al.*, 1989; *van Keulen et al.*, 1989]. In our study, we examined the $N_{area} - A_{max}$ relationship for boreal forest vegetation by sampling branches from the overstory and understory and indeed found a weak but general relationship between N_{area} and A_{max} when all five of our stands were combined ($r = 0.51$, $p < 0.0001$) for IFC-2 and IFC-3.

We also found exceptions to the general $N_{area} - A_{max}$ relationship. A negative relationship between N_{area} and A_{max} was found for jack pine during IFC-1 (Figure 8, Table 2). We suggest that higher rates of bud respiration in the upper canopy than the lower canopy may be responsible for this reversed relationship. We observed that there were both more and larger buds in the upper canopy than in the lower canopy of the jack pine stands. As well, buds in the upper canopy broke earlier than the ones in the lower canopy. Thus we hypothesize that differences in bud respiration rates between canopy levels may have surpassed the differences in photosynthesis. Because black spruce has much smaller buds, the respiration effect may not have been strong enough to reverse the $N_{area} - A_{max}$ profile.

Another partial exception to the general $N_{area} - A_{max}$ relationship during IFC-1 was found for the aspen stand when N_{area} for the understory alder was higher than it was for the overstory aspen. Nevertheless, the $N_{area} - A_{max}$ relationship still held, since alder had both higher N_{area} and higher A_{max} than aspen during IFC-1.

There was a major difference in the $N_{area} - A_{max}$ relationship between the aspen and the conifer stands (Figure 7a). All canopies had a similar range of N_{area} (Figures 7a and 12b), but aspen tended to have a higher A_{max} (Figures 7a and 12a) and
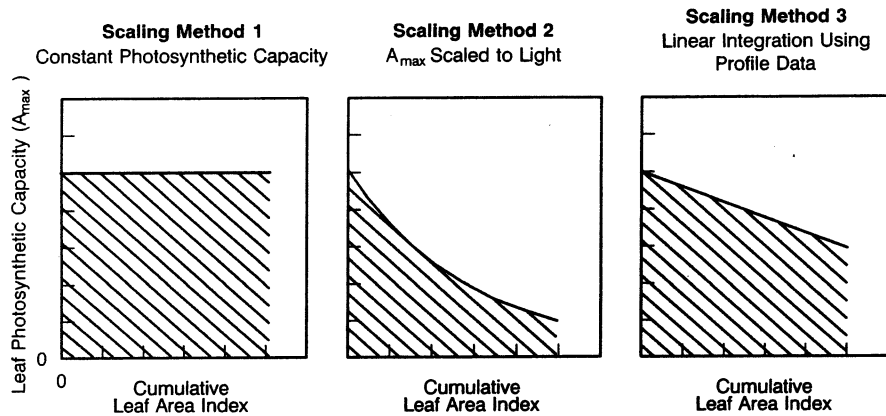
Figure 13. Three simple methods of scaling leaf-level photosynthetic capacity to the canopy. (a) Method 1 assumes constant A_{max} through the canopy. (b) Method 2 assumes a proportional change in PAR and A_{max}, i.e., $A_{max} = A_{max0}$ (PAR/PAR_0), where A_{max} and PAR are leaf photosynthetic capacity and photosynthetically active radiation at a given level within the canopy, respectively; A_{max0} and PAR_0 are leaf photosynthetic capacity and PAR at the top of the canopy, respectively. (c) Method 3 uses the linear relationship between A_{max} and cumulative leaf area index from the top of the canopy as developed from our data. The hatched area under each curve represents the canopy photosynthetic capacity ($A_{can-max}$) calculated using the corresponding scaling method. Calculations do not include the photosynthetic capacity of the ground cover.

therefore higher nitrogen use efficiency (NUE) (Figure 12c). This result implies that aspen probably allocated a greater proportion of leaf nitrogen to photosynthetic function and a relatively smaller proportion to leaf structure than did the conifers. This interpretation is consistent with the morphological differences between the aspen and the conifer foliage. This is further supported by the pattern that occurred when the relationship between N_{area} and A_{max} was examined as a percentage of the maximum value at the top of the canopy, i.e., $\%N_{max0}$ and $\%A_{max0}$ (Figure 10a). The aspen stand showed a one-to-one relationship, i.e., a 20% decline in $\%N_{max0}$ resulted in a corresponding 20% decline in $\%A_{max0}$. The conifers, on the other hand, showed a smaller decline in $\%A_{max0}$ for a given decline in $\%N_{max0}$, indicating that part of the decline in nitrogen was from the nonphotosynthetic nitrogen component. Thus the proportion of foliar nitrogen allocated to photosynthetic function in the conifers appeared to increase with canopy depth and varied among canopy types.

Although A_{max} declined linearly with increasing depth in the canopy (equations (2), (3), and (4)), it declined at a much slower rate than did %PAR (Figure 10b). Thus our analysis does not support the assumption in the scaling algorithms described by *Sellers et al.* [1992, 1996] and *Kull and Jarvis* [1995], where A_{max} is assumed to decline with canopy depth at the same rate as %PAR. There are several reasons why this can occur. For example, the upper canopy leaves of boreal forest trees do not have the genetic capacity to take full advantage of the light levels that occur during the summer months. Typical maximum PAR levels during sunny days in the summer at our sites were between 1600 and 1900 $\mu mol\ m^{-2}\ s^{-1}$. Photosynthesis, on the other hand, attains light saturation between 600 and 800 $\mu mol\ m^{-2}\ s^{-1}$ for the aspen, jack pine, and black spruce in our study area (unpublished data). Thus a 40% decline in PAR from 1500 to 900 $\mu mol\ m^{-2}\ s^{-1}$ within a canopy should not be expected to result in any decrease in A_{max} since photosynthesis would still be light-saturated. PAR levels at the bottom of the canopy, on the other hand, are likely to be limiting to photosynthesis (Figure 3).

Another potential reason for the nonproportional scaling of

%PAR and $\%A_{max0}$ is that the foliage within the canopy maintained a higher A_{max} so that it could take advantage of the higher than average light levels that regularly occur on sunny days (Figure 1). In this case, the foliage would not scale its A_{max} to the average light condition but perhaps to the maximum light level at a given canopy level. However, acclimating A_{max} to maximum light levels would not be efficient if nitrogen concentrations got so high that respiratory losses during periods of low light and darkness exceeded the potential gain during periods of high light. Additionally, because stomatal conductance is very closely related to photosynthetic capacity (Figure 9) [*Wong et al.*, 1979], the way in which leaf A_{max} scales to resource availability can also be directly related to water and heat fluxes.

There was considerable unexplained variation in the relationship between %PAR, N_{area}, and A_{max}. The correlation coefficients were generally low (0.4–0.6), although they are similar to those reported by *Field* [1991] for a range of different plant communities. Despite the considerable amount of unexplained variation, our data do show that leaf A_{max} tended to scale to resource availability across the different boreal forest cover types but not exactly in the way suggested by the functional convergence hypothesis (Figure 10b). This scaling to resource availability was particularly striking when both PAR and A_{max} were expressed as relative values, i.e., %PAR versus $\%A_{max0}$ (Figure 10b). In this case, all five stands had very similar relationships (Figure 10b). The similarity of this relationship for the different sites suggests that simplified methods of scaling leaf photosynthesis to the canopy may be possible using a reduced number of parameters to describe all boreal forest canopies.

To demonstrate impacts that different assumptions about the vertical distribution of leaf photosynthetic capacity (A_{max}) could have on the scaling of A_{max} to the canopy ($A_{can-max}$), we used a simple scaling technique to calculate $A_{can-max}$ for two different theoretical vertical distributions of A_{max} within the canopy (Methods 1 and 2, Figure 13) and for the actual A_{max} distribution as determined from our measurements (Method 3, Figure 13). With more detailed information on stand architec-

Table 3. Scaling Photosynthetic Capacity From Leaf (A_{max}) to Canopy ($A_{can-max}$)

Stand	A_{max0}	LAI	Method 1, ($A_{max0} \times$ LAI)	Method 2, ($A_{max0} \times f$PAR$/k_L$)	Method 3, ($\int A_{max}$) (linear)
NSA-OASP	9.44	2.2	20.8	8.3	14.5
NSA-UBS	3.54	4.2	14.2	5.1	13.2
NSA-OBS	3.39	2.4	8.5	4.3	7.6
NSA-OJP	4.43	1.1	4.9	2.9	4.6
NSA-YJP	4.14	0.9	3.7	2.5	3.6

Note that A_{max0} is A_{max} at the top of a canopy. A_{max0} and A_{max} values (μmol CO_2 m^{-2} leaf s^{-1}) are taken from our data and are on a hemisurface leaf area basis. LAI values are also a hemisurface basis and are from allometric data collected by BOREAS TE-6 team. Canopy photosynthetic capacity values ($A_{can-max}$) are in μmol CO_2 m^{-2} ground s^{-1}. See Discussion and Figure 13 for further details on the scaling methods.

ture, more sophisticated scaling methods could be used [e.g., *Baldocchi*, 1993; *Norman*, 1993]. However, the simple technique that we used is sufficient for our current purpose.

In Method 1 (Figure 13), A_{max} is assumed to be constant through the canopy [e.g., *Sellers et al.*, 1987], and thus $A_{can-max}$ is calculated as

$$A_{can-max} = L_t \times A_{max0} \qquad (7)$$

where A_{max0} is the photosynthetic capacity of foliage in the upper canopy as measured in the current study, and L_t is total leaf area index (LAI) for the canopy. Only overstory LAI values were available for these sites, so the scaling was conducted accordingly.

In Method 2 (Figure 13), A_{max} is assumed to decrease proportionally to %PAR [*Sellers et al.*, 1992, 1996; *Kull and Jarvis*, 1995], and $A_{can-max}$ is thus calculated as

$$A_{can-max} = (A_{max0} f\text{PAR}/k_L) \qquad (8)$$

where fPAR is

$$f\text{PAR} = [1 - e^{-k_L L_i}] \qquad (9)$$

and k_L is the extinction coefficient for light with cumulative LAI defined as

$$k_L = (k_D D/L_i) \qquad (10)$$

and D is depth into the canopy.

In Method 3 (Figure 13), $A_{can-max}$ was calculated on the basis of our actual profile data by substituting $k_L L$ for $k_D D$ in (1) and (2). Then for each stand we integrated A_{max} as a function of cumulative LAI (L_{cum}) to give us $A_{can-max}$ for the total canopy LAI (L_t),

$$A_{can-max} = \int_0^{L_i} [p - q(L_{cum})] \, d(L) = p(L_i) - [q(L_i)^2/2] \qquad (11)$$

where p and q are the parameters arising from combining the regression parameters from the earlier substitutions. The first term on the right-hand side of the above equation calculates $A_{can-max}$ assuming a constant A_{max} with depth, and the second term is an adjustment factor that takes into account the vertical decrease in A_{max} that was measured in each of our respective stands.

The scaling method that was based on our profile measurements (Method 3) gave estimates much closer to Method 1 (i.e., constant A_{max} through the canopy) than to Method 2 (proportional scaling of A_{max} to %PAR) (Table 3). This is

reasonable since despite the large decreases in %PAR, %A_{max0} did not decrease below 75% for any stand and was normally well above 80% (Figure 10b). The differences in calculated $A_{can-max}$ ranged from 3 to 43% between Methods 1 and 3 for the five stands and from 31 to 61% between Methods 2 and 3 (Table 3). If differences in PAR between different canopy levels were taken into account, the differences in the rates of light-limited photosynthesis might be smaller than the differences in $A_{can-max}$ for the different scaling methods. Method 2 implies that photosynthesis for the entire canopy is light-saturated when the top leaf is light-saturated, while Methods 1 and 3 imply that light saturation for the canopy occurs at higher PAR levels than it does for the top leaf. *Leuning et al.* [1995] conducted an analysis of the consequences of constant versus proportionally declining A_{max} on carbon gain and found that the difference between the two assumptions was generally less than 10%.

NDVI and simple ratio are two common vegetation indices measured by remote sensing and are strongly correlated to the PAR absorbed by a plant canopy. The estimate of $A_{can-max}$ using our profile data (Method 3) was significantly correlated with both the NDVI and the simple ratio remote sensing indices ($r = 0.93$ and 0.83, respectively; Figures 14a, 14b). The reason for the lower correlation with simple ratio is likely the apparent instability of the simple ratio in dense canopies; that is, small changes in the red reflectance in the denominator can result in large changes in the simple ratio.

Working with miniature conifer canopies where photosynthetic potential was artificially manipulated independently of leaf area and light absorption capacity, *Yoder and Waring* [1994] found that NDVI calculated by using a narrow green wave band (565–575 nm) had a higher correlation with photosynthetic potential than NDVI calculated with a narrow red wave band (671–674 nm). The high correlations found in our study between NDVI calculated by using a red wave band and $A_{can-max}$ are likely due to the close association between the amount of radiation absorbed by a unit of ground area and its photosynthetic potential. Nevertheless, the method used to scale up to $A_{can-max}$ had a large effect on the slope of the relationship between NDVI and $A_{can-max}$ (Figure 15), particularly when Method 2 is compared with the other methods. Thus the assumptions used in scaling from leaf to canopy can have a large impact on predictions of canopy photosynthetic capacity and possibly actual canopy photosynthesis as well. How much of an influence this might have on estimates of the regional carbon budget for the boreal forest biome remains to be determined.
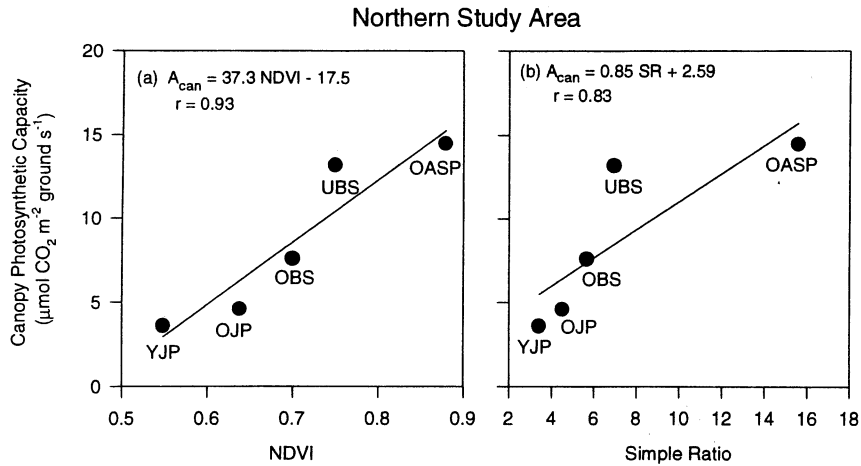
Northern Study Area

Figure 14. Canopy photosynthetic capacity ($A_{\text{can-max}}$) as calculated by Method 3 (see Figure 13 and Discussion section) in relation to (a) NDVI and (b) simple ratio.

Ogunjemiyo et al. [this issue] showed that CO_2 flux measurements made with the Twin Otter flux aircraft were strongly correlated to the simple ratio vegetation index for the BOREAS northern study area, the BOREAS southern study area, and a 500 km regional transect between the two areas. The fact that both CO_2 flux and $A_{\text{can-max}}$ (Figure 14) have strong positive correlations with the simple ratio and/or the NDVI vegetation indices indicates that areas of the boreal forest with a higher photosynthetic capacity should also have higher CO_2 flux and that both have the potential to be estimated by remote sensing.

References

Abidine, A. Z. E., J. D. Stewart, P. Y. Bernier, and A. P. Plamondon, Diurnal and seasonal variations in gas exchange and water relations of lowland and upland black spruce ecotypes, *Can. J. Bot.*, *73*, 716–722, 1995.

Abrams, M. C., and S. A. Mostoller, Gas exchange, leaf structure and nitrogen in contrasting successional tree species growing in open and understory sites during a drought, *Tree Physiol.*, *15*, 361–370, 1995.

Baldocchi, D. D., Scaling water vapor and carbon dioxide exchange from leaves to a canopy: Rules and tools, in *Scaling Physiological Processes: Leaf to Globe*, edited by J. R. Ehleringer and C. B. Field, pp. 77–114, Academic, San Diego, Calif., 1993.

Bloom, A. J., F. S. Chapin III, and H. A. Mooney, Resource limitation in plants—An economic analogy, *Annu. Rev. Ecol. Syst.*, *16*, 363–392, 1985.

Brand, D. G., Estimating the surface area of spruce and pine foliage from displaced volume and length, *Can. J. For. Res.*, *17*, 1305–1308, 1987.

Brooks, J. R., D. G. Sprugel, and T. M. Hinckley, The effects of light acclimation during and after foliage expansion on photosynthesis of *Abies amabilis* foliage within the canopy, *Oecologia*, *107*, 21–32, 1996.

Charles-Edwards, D. A., H. Stutzel, R. Ferraris, and D. F. Beech, An analysis of spatial variation in the nitrogen content of leaves from different horizons within a canopy, *Ann. Bot.*, *60*, 421–426, 1987.

Chen, J. M., Optically-based methods for measuring seasonal variation of leaf area index in boreal conifer stands, *Agric. For. Meteorol.*, *80*, 135–163, 1996.

Chen, J. M., and T. A. Black, Measuring leaf area index of plant canopies with branch architecture, *Agric. For. Meteorol.*, *57*, 1–12, 1991.

Dang, Q. L., H. A. Margolis, M. R. Coyea, M. Sy, and G. J. Collatz, Regulation of branch-level gas exchange of boreal trees: Role of shoot water potential and vapor pressure difference, *Tree Physiol.*, *17*, 521–536, 1997.

DeJong, T. M., and J. F. Doyle, Seasonal relationships between leaf
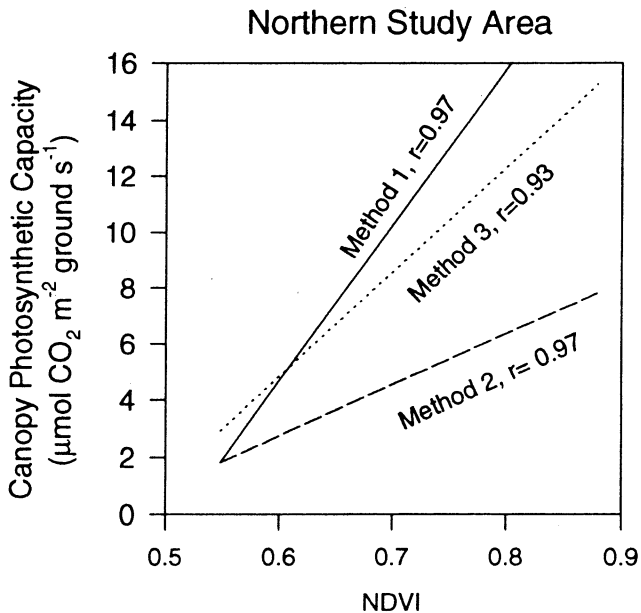
Northern Study Area

Figure 15. Relationship between NDVI and canopy photosynthetic capacity ($A_{\text{can-max}}$) calculated from three different scaling methods (see Figure 13 and Discussion section). Method 1 (constant A_{max}): $A_{\text{can-max}} = (55.5\ \text{NDVI}) - 28.6$; Method 2 ($A_{\text{max}}$ scaled to %PAR): $A_{\text{can-max}} = (18.1\ \text{NDVI}) - 8.1$; Method 3 (linear integration using profile data): $A_{\text{can-max}} = (37.3\ \text{NDVI}) - 17.5$.

nitrogen content (photosynthetic capacity) and leaf canopy light exposure in peach (*Prunus perspicata*), *Plant Cell Environ., 8*, 701–706, 1985.

Draper, H. R., and H. Smith, *Applied Regression Analysis*, 2nd ed., 700 pp., John Wiley, New York, 1981.

Ellsworth, D. S., and P. B. Reich, Canopy structure and vertical patterns of photosynthesis and related leaf traits in a deciduous forest, *Oecologia, 96*, 169–178, 1993.

Evans, J. R., Photosynthesis and nitrogen relationships in leaves of C₃ plants, *Oecol., (Berlin), 78*, 9–19, 1989.

Evans, J. R., and G. D. Farquhar, Modelling canopy photosynthesis from the biochemistry of the C₃ chloroplast, in *Modelling Crop Photosynthesis—From Biochemistry to Canopy*, edited by K. J. Boote and R. S. Loomis, pp. 1–15, *Spec. Publ. 19*, Crop Sci. Soc. of Am./Crop Sci. Soc. of Am. and Am. Soc. of Agron., Madison, Wis., 1991.

Farquhar, G. D., Models of integrated photosynthesis of cells and leaves, *Philos. Trans. R. Soc. London, Ser. B, 323*, 357–367, 1989.

Field, C. B., Ecological scaling of carbon gain to stress and resource availability, in *Response of Plants to Multiple Stresses*, edited by H. A. Mooney, W. E. Winner, and E. J. Pell, pp. 35–65, Academic, San Diego, Calif., 1991.

Field, C. B., and H. A. Mooney, Leaf age and seasonal effects on light, water, and nitrogen use efficiency in a California shrub, *Oecologia, 56*, 348–355, 1983.

Field, C. B., and H. A. Mooney, The photosynthesis–nitrogen relationship in wild plants, in *On the Economy Plant Form and Function*, edited by T. J. Givnish, pp. 25–55, Cambridge Univ. Press, New York, 1986.

Field, C. B., J. Merino, and H. A. Mooney, Compromises between water-use efficiency and nitrogen-use efficiency in five species of California evergreens, *Oecologia, 60*, 384–389, 1983.

Hirose, T., and M. J. A. Werger, Maximizing daily canopy photosynthesis with respect to the leaf nitrogen allocation pattern in the canopy, *Oecologia, 72*, 520–526, 1987a.

Hirose, T., and M. J. A. Werger, Nitrogen use efficiency in instantaneous and daily photosynthesis of leaves in the canopy of a *Solidago altissima* stand, *Physiol. Plant., 70*, 215–222, 1987b.

Hirose, T., M. J. A. Werger, T. L. Pons, and J. W. A. van Rheenen, Canopy structure and leaf nitrogen distribution in a stand of *Lysimachia vulgaris* L. as influenced by stand density, *Oecologia, 77*, 145–150, 1988.

Hirose, T., M. J. A. Werger, and J. W. A. van Rheenen, Canopy development and leaf nitrogen distribution in a stand of *Carex acutifomis*, *Ecology, 70*, 1610–1618, 1989.

Hollinger, D. Y., Canopy organization and foliage photosynthetic capacity in a broad-leaved evergreen montane forest, *Funct. Ecol., 3*, 53–62, 1989.

Hollinger, D. Y., Optimality and nitrogen allocation in a tree canopy, *Tree Physiol., 16*, 627–634, 1996.

Jupp, D. L. B., and A. H. Strahler, A hotspot model for leaf canopies, *Remote Sens. Environ., 38*, 193–210, 1991.

Kull, O., and P. G. Jarvis, The role of nitrogen in a simple scheme to scale up photosynthesis from leaf to canopy, *Plant Cell Environ., 18*, 1174–1182, 1995.

Landsberg, J. J., *Physiological Ecology of Forest Production*, 198 pp., Academic, San Diego, Calif., 1986.

Leuning, R., F. M. Kelliher, D. G. G. dePury, and E.-D. Schulze, Leaf nitrogen, photosynthesis, conductance and transpiration: Scaling from leaves to canopies, *Plant Cell Environ., 18*, 1183–1200, 1995.

Loechel, S. E., C. L. Walthall, E. Brown de Colstoun, J. Chen, B. L. Markham, and J. Miller, Variability of boreal forest reflectances as measured from a helicopter platform, *J. Geophys. Res.*, this issue.

Luo, Y., C. B. Field, and H. A. Mooney, Predicting responses of photosynthesis and root fraction to elevated [CO₂]: Interactions among carbon, nitrogen, and growth, *Plant Cell Environ., 17*, 1195–1204, 1994.

Markham, B. L., F. Wood, and S. P. Ahmad, Radiometric calibration of the reflective band of NS001-Thematic Mapper Simulator (TMS) and Modular Multiband Radiometers (MMR), in *Recent Advances in Sensors, Radiometry, and Data Processing for Remote Sensing, Proc. SPIE Int. Soc. Opt. Eng., 24*, 96–108, 1988.

Messier, C., and P. Puttonen, Spatial and temporal variation in the light environment of developing Scots pine stands: The basis for a quick and efficient method of characterizing light, *Can. J. For. Res., 25*, 343–354, 1995.

Middleton, E. M., J. H. Sullivan, B. D. Bovard, A. J. Deluca, S. S.

Chan, B. D. Bovard, A. J. DeLuca, and T. A. Cannon, Seasonal variability in foliar characteristics and physiology for boreal forest species at the five Saskatchewan tower sites during the 1994 Boreal Ecosystem-Atmosphere Study (BOREAS), *J. Geophys. Res.*, this issue.

Mitchell, A. K., and T. M. Hinckley, Effects of foliar nitrogen concentration on photosynthesis and water use efficiency in Douglas-fir, *Tree Physiol., 12*, 403–410, 1993.

Mooney, H. A., and S. L. Gulmon, Environmental and evolutionary constraints on photosynthetic characteristics of higher plants, in *Topics in Plant Population Biology*, edited by O. T. Solbrig, S. Jain, G. B. Johnson, and P. H. Raven, pp. 316–337, Columbia Univ. Press, New York, 1979.

Mooney, H. A., and S. L. Gulmon, Constraints on leaf structure and function in relation to herbivory, *BioScience, 32*, 198–206, 1982.

Neter, J., W. Wasserman, and M. H. Kutner, *Applied Linear Statistical Models: Regression Analysis of Variance and Experimental Designs*, 3rd ed., 1181 pp., Irwin, Inc., Burr Ridge, Ill., 1990.

Norman, J. M., Modeling the complete crop canopy, in *Modification of the Aerial Environments of Plants*, edited by B. J. Barfield and J. F. Gerber, pp. 249–277, Am. Soc. Agric. Eng., St. Joseph, Mich., 1979.

Norman, J. M., Scaling processes between leaf and canopy levels, in *Scaling Physiological Processes: Leaf to Globe*, edited by J. R. Ehleringer and C. B. Field, pp. 41–76, Academic, San Diego, Calif., 1993.

Ogunjemiyo, S., P. H. Schuepp, J. I. MacPherson, and R. L. Desjardins, Analysis of flux maps versus surface characteristics from Twin Otter grid flights in BOREAS 1994, *J. Geophys. Res.*, this issue.

Otterman, J., and T. W. Brakke, Multiple versus single scattering: Assessment of magnitude, *Appl. Opt., 30*, 1562–1566, 1991.

Pons, R. L., and R. W. Pearcy, Nitrogen reallocation and photosynthetic acclimation in response to partial shading in soybean plants, *Physiol. Plant., 92*, 636–644, 1994.

Reich, P. B., M. B. Walters, D. S. Ellsworth, and C. Uhl, Photosynthesis-nitrogen relations in Amazonian tree species, I, Patterns among species and communities, *Oecologia, 97*, 62–72, 1994.

Sarndal, C.-E., B. Swensson, and J. Wretman, *Model Assisted Survey Sampling*, 509 pp., Springer-Verlag, New York, 1992.

Schulze, E.-D., F. M. Kelliher, C. Korner, J. Lloyd, and R. Leuning, Relationships among maximum stomatal conductance, ecosystem surface conductance, carbon assimilation rate and plant nitrogen nutrition: A global ecology scaling exercise, *Ann. Rev. Ecol. Syst., 25*, 629–660, 1994.

Seeman, J. R., T. D. Sharkey, and J. L. Wang, and C. B. Osmond, Environmental effects on photosynthesis, nitrogen-use efficiency and metabolite pools in leaves of sun and shade plants, *Plant Physiol., 84*, 796–802, 1987.

Sellers, P. J., Canopy reflectance, photosynthesis, and transpiration, II, The role of biophysics in the linearity of their interdependence, *Remote Sens. Environ., 21*, 143–183, 1987.

Sellers, P. J., J. A. Berry, G. J. Collatz, C. B. Field, and F. G. Hall, Canopy reflectance, photosynthesis and transpiration, III, A reanalysis using improved leaf models and a new canopy integration scheme, *Remote Sens. Environ., 42*, 187–216, 1992.

Sellers, P. J., et al., The Boreal Ecosystem-Atmosphere Study (BOREAS): An overview and early results from the 1994 field year, *Bull. Am. Meteorol. Soc., 76*, 1549–1577, 1995.

Sellers, P. J., D. A. Randall, G. J. Collatz, J. A. Berry, C. B. Field, D. A. Dazlich, C. Zhang, and G. D. Collelo, A revised land surface parameterization (SiB2) for atmospheric GCMs, 1, Model formulation, *J. Clim., 9*, 676–705, 1996.

Smith, N. J., J. M. Chen, and T. A. Black, Effects of clumping on estimates of stand leaf area index using the LI-COR LAI-2000, *Can. J. For. Res., 23*, 1940–1943, 1993.

Tan, W. X., and G. D. Hogan, Limitations to net photosynthesis as affected by nitrogen status in jack pine (*Pinus banksiana* Lamb.) seedlings, *J. Exp. Bot., 46*, 407–413, 1995.

Thompson, W. A., L. K. Huang, and P. E. Kriedemann, Photosynthetic response to light and nutrients in sun-tolerant and shade-tolerant rainforest trees, II, Leaf gas exchange and component processes of photosynthesis, *Aust. J. Plant Physiol., 19*, 19–42, 1992.

van Keulen, H., J. Goudriaan, and N. G. Seligman, Modelling the effects of nitrogen on canopy development and crop growth, in *Plant Canopies: Their Growth, Form and Function*, edited by G. Russell, B. Marshall, and P. G. Jarvis, pp. 83–104, Cambridge University Press, New York, 1989.

Verhoef, W., Light scattering by leaf layers with application to canopy reflectance modeling: The SAIL model, *Remote Sens. Environ., 33,* 97–112, 1984.

von Caemmerer, S., and G. D. Farquhar, Some relationships between biochemistry of photosynthesis and the gas exchange of leaves, *Planta, 153,* 376–387, 1981.

Walters, M. B., and P. B. Reich, Response of *Ulmus americana* seedlings to varying nitrogen and water status, 1, Photosynthesis and growth, *Tree Physiol., 5,* 159–172, 1989.

Walthall, C. L., D. L. Williams, B. L. Markham, J. E. Kalshoven, and R. F. Nelson, Development and present configuration of the NASA GSFC/WFF helicopter based remote sensing system, *Proc. IGARSS'96, IEEE, 3,* 1797–1799, 1996.

Wang, Y. P., and P. G. Jarvis, Influences of crown structural properties on PAR absorption, photosynthesis and transpiration in Sitka spruce: Application of a model (MAESTRO), *Tree Physiol., 7,* 297–316, 1991.

Wong, S. C., I. R. Cowan, and G. D. Farquhar, Stomatal conductance correlates with photosynthetic capacity, *Nature, 282,* 424–426, 1979.

Yoder, B. J., and R. H. Waring, The normalized difference vegetation index of small Douglas-fir canopies with varying chlorophyll concentrations, *Remote Sens. Environ., 94,* 81–91, 1994.

Yue, D., Y. Desjardins, M. Lamarre, and A. Gosselin, Photosynthesis and transpiration of *in vitro* cultured asparagus plantlets, *Sci. Hortic. Amsterdam, 49,* 9–14, 1992.

G. J. Collatz, Biospheric Sciences Branch, Code 923, Building 22, NASA Goddard Space Flight Center, Greenbelt, MD 20771.

M. R. Coyea and H. A. Margolis, Centre de Recherche en Biologie Forestière, Pavillon Abitibi-Price, Université Laval, Sainte-Foy, Québec, Canada G1K 7P4. (fax: (418) 656-3551)

Q. L. Dang, Lakehead University, Faculty of Forestry, 955 Oliver Road, Thunder Bay, Ontario, Canada P7B 5E1. (e-mail: qdang@skylakeheadU.ca)

M. Sy, Institute of Biology, Biology Department, Carleton University, Ottawa, Ontario, Canada K1S 5B6.

C. L. Walthall, USDA/ARS, Remote Sensing Research Laboratory, BARC West, Building 007, Beltsville, MD 20705.